Techniques and Strategies for Minimizing Reconstruction Artifacts in Extended FOV CT used for Radiation Therapy Treatment Planning

S Scarboro[1]; A Polemi[2]; E Aliotta[1]; P Collins[2]
[1]University of Virginia Department of Radiation Oncology
[2]University of Virginia Department of Radiology and Medical Imaging

JULY 12–16 2020 VIRTUAL
JOINT AAPM | COMP MEETING
EASTERN TIME [GMT-4]

INTRODUCTION

Siemens CT scanners are becoming more common in Radiation Oncology settings, likely due to attractive options such as dual energy. Treatment planning CT datasets often require extended field of view (eFOV) reconstructions due to patient size, positioning, or large immobilization devices. However, eFOV reconstructions inherently suffer from artifacts from incomplete data sampling, which make the critical task of accurate edge definition and landmark placement challenging. The presence of these artifacts may alter the appearance of target volumes depending on their position within the patient and relative to the edge of the bore [1, 2]. The motivation for this work was to investigate clinically significant artifacts which appeared in our clinic and identify practical strategies for minimizing them through manipulation of scanning protocol parameters.

AIM

The purpose of this study was to evaluate techniques and strategies for minimizing reconstruction artifacts, such as image distortion and incorrect HU values, in the extended FOV of Siemens CT scanners used for treatment planning.

METHODS

An anthropomorphic body phantom with added fat layers was scanned on a Siemens Definition Edge (Siemens Healthineers, Erlangen, Germany) using 6 different protocols with varied pitch, slice thickness, acquisition configuration, and scan direction, as outlined in Table 1. Four phantom positions (2 inside the scanning FOV (sFOV), 2 outside the sFOV) were examined to determine the impact of eFOV reconstruction on preserving image integrity and HU values. Distortion of the phantom external contour was investigated by evaluating the phantom diameter using profiles from axial slices using a MATLAB routine. ROIs were placed in sections of fat, soft tissue, and bone for computation of mean HU. All values were compared to measurements made with the phantom positioned at isocenter and reported as a function of phantom position and protocol.

Protocol	Pitch	Acquisition Configuration	Slice Thickness (mm)
1	0.35	128x0.6	1
2	0.6	32x1.2	3
3	0.35	32x1.2	3
4	0.35	128x0.6	3
5	0.6	128x0.6	1
6	0.6	128x0.6	3

Table 1: Varied technical scan parameters for the protocols tested. All protocols used 120 kVp, 200 mA, and 1 second rotation time. Scans were completed in both cranial-caudal and caudal-cranial directions.

RESULTS

Figure 1 demonstrates the radial diameters drawn on the axial slices and used to evaluate the degree of spatial distortion at the 4 phantom positions. The differences in diameter relative to isocenter, averaged over all phantom positions, were minimized for protocols with a lower pitch; the maximum error observed, 41.6 mm, was reduced to 25.9 mm. Little dependence was observed for acquisition configuration or reconstructed slice thickness. The observed errors were greatest for the slice nearest to the transition between air and fat, which changed with scan direction. Figures 2 and 3 illustrate the geometric distortion that occurs at the air/tissue boundary. Mean HU values for positions outside the sFOV were found to differ greatly from those at isocenter, with little dependence on protocol. The average HU value difference for tissue and fat, across all protocols, from isocenter to maximum offset position, was 58 mm±3.9 mm and 23 mm±4.0 mm, respectively.

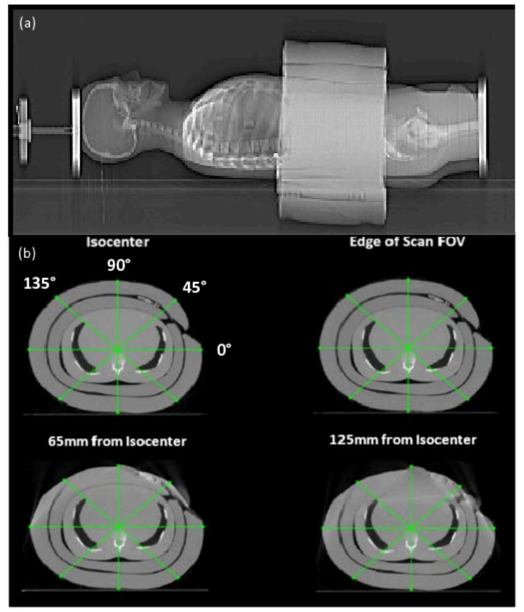

Figure 1: (a) Lateral topogram image of the anthropomorphic phantom with fat layers. (b) Axial slices of the phantom for the 4 positions tested: isocenter, edge of scan FOV, 65 mm from isocenter, and 125 mm from isocenter. The green lines indicate the 4 radial diameters used to evaluate spatial distortion. The horizontal diameter was designated as 0 degrees. The other diameters were drawn at 45, 90, and 135 degrees, with respect to zero, as shown. The spatial distortion of the axial images can be appreciated for the phantom positions outside the scan FOV.

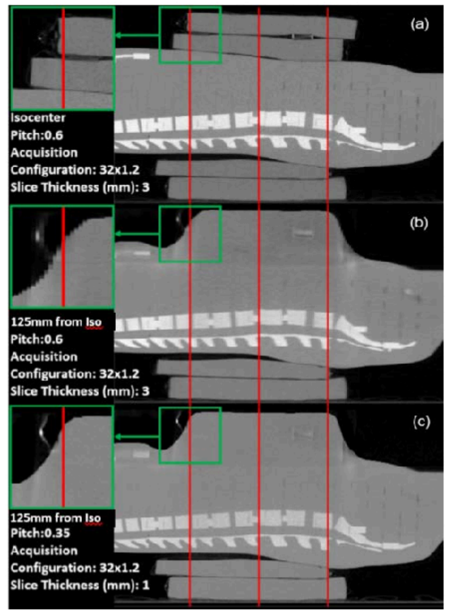

Figure 2: Sagittal slices of the anthropomorphic phantom. (a) Phantom positioned at isocenter, (b-c) phantom positioned at maximum offset from isocenter. (b) Demonstrates the protocol with the maximum spatial distortion while (c) demonstrates the protocol with the minimum. The red lines represent the location of the slices where the phantom diameters were evaluated.

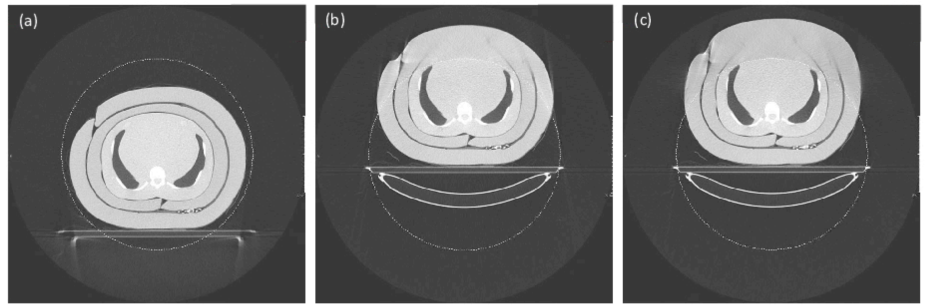

Figure 3: Axial slices of the anthropomorphic phantom acquired with protocol 1 demonstrating the impact scan direction has on spatial distortion. (a) Phantom positioned at isocenter, scanned cranial-caudal. (b-c) Phantom positioned 125 mm from isocenter, (b) scanned cranial-caudal and (c) scanned caudal-cranial. The dotted white lines represent the sFOV.

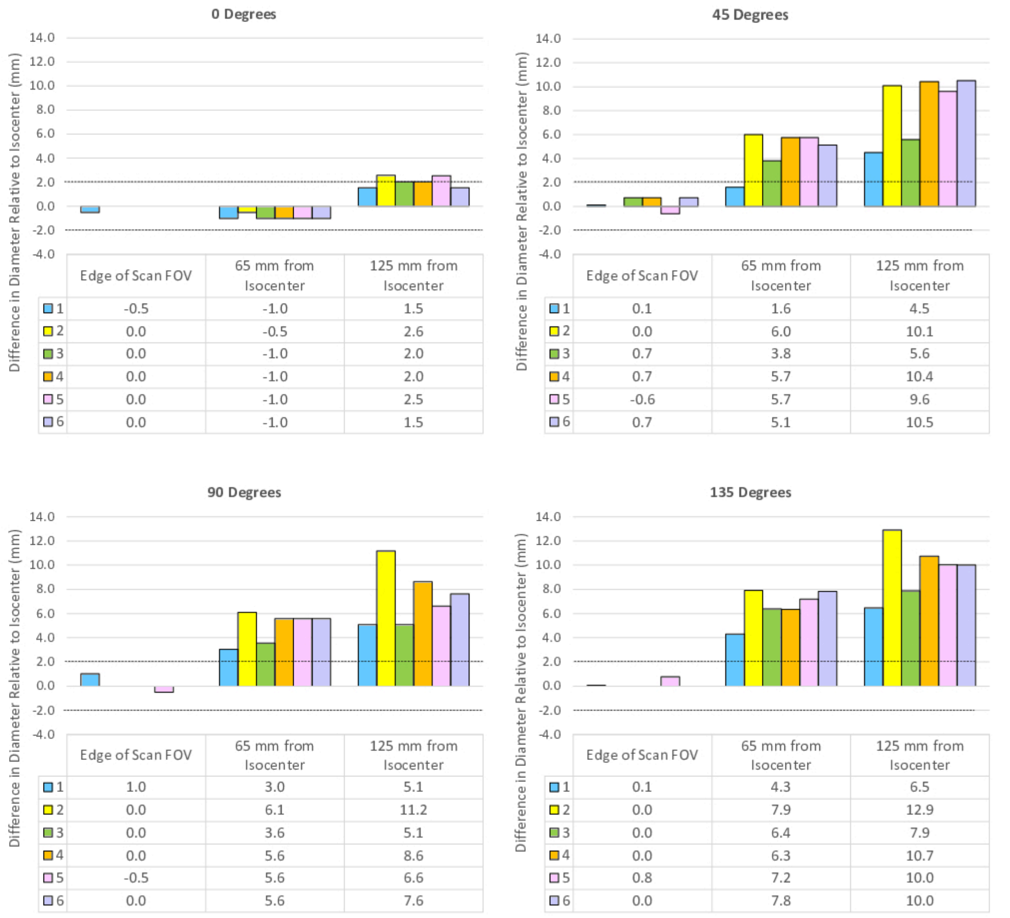

0 Degrees

	Edge of Scan FOV	65 mm from Isocenter	125 mm from Isocenter
1	-0.5	-1.0	1.5
2	0.0	-0.5	2.6
3	0.0	-1.0	2.0
4	0.0	-1.0	2.0
5	0.0	-1.0	2.5
6	0.0	-1.0	1.5

45 Degrees

	Edge of Scan FOV	65 mm from Isocenter	125 mm from Isocenter
1	0.1	1.6	4.5
2	0.0	6.0	10.1
3	0.7	3.8	5.6
4	0.7	5.7	10.4
5	-0.6	5.7	9.6
6	0.7	5.1	10.5

90 Degrees

	Edge of Scan FOV	65 mm from Isocenter	125 mm from Isocenter
1	1.0	3.0	5.1
2	0.0	6.1	11.2
3	0.0	3.6	5.1
4	0.0	5.6	8.6
5	-0.5	5.6	6.6
6	0.0	5.6	7.6

135 Degrees

	Edge of Scan FOV	65 mm from Isocenter	125 mm from Isocenter
1	0.1	4.3	6.5
2	0.0	7.9	12.9
3	0.0	6.4	7.9
4	0.0	6.3	10.7
5	0.8	7.2	10.0
6	0.0	7.8	10.0

Figure 4: Difference in phantom diameter (in mm) relative to diameter measured with phantom positioned at isocenter, averaged across all 3 slices (indicated by red lines in Figure 2). The dotted lines represent ±2 mm, which is a typical tolerance used for planning.

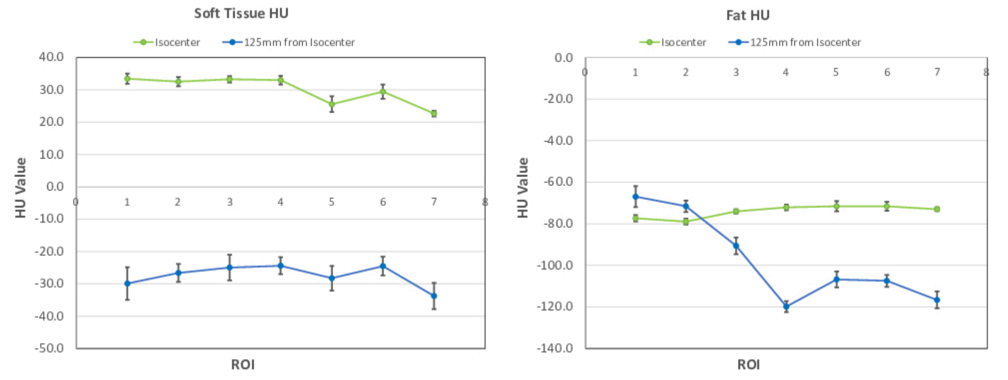

Figure 5: Mean HU values, for soft tissue and fat, averaged across all tested protocols for isocenter and maximum phantom offset position (125mm from isocenter). The small error bars demonstrate little dependence on protocol.

CONCLUSIONS

The results of this study demonstrate varying appearance of artifacts using eFOV reconstructions based on phantom position, inside or outside of the scanning FOV, for the same acquisition protocols. The worst artifact (qualitatively) was seen for the two reconstructions for phantom positions at 65 mm from isocenter and 125 mm from isocenter. For several cases, we measured a geometric difference of more than 10 mm in phantom diameter. Oblique angles of the axial slices suffered worse geometric differences compared to the 0 and 90 degree profiles. We found that selection of pitch has the greatest impact on reducing eFOV image distortion. Sharp transitions between air and tissue amplify the distortions, however, these can be partially reduced by changing scan direction (tissue-air vs. air-tissue). Scanning in a direction such that a difference in phantom 'thickness' is approached from tissue rather than air reduces the artifact.

HU values have little dependence on protocol parameters. For phantom positions outside the sFOV, the difference in HU value approached 60HU for soft tissue and around 23 for fat.

Future work includes investigating the effect of reconstruction kernel on HU value and image distortion. All of the results presented here were reconstructed using the Siemens Br38 kernel. The sharpness or smoothness of the kernel used, along with a lower pitch, may further reduce artifacts and increase HU accuracy. We aim to apply these findings to our current clinical protocols and further evaluate with patient studies.

ACKNOWLEDGEMENTS

The authors would like to thank Siemens, especially Guillaume Grousset and Jainil Shah, for useful conversations regarding the discovery of artifacts and subsequent investigation.

REFERENCES

1. Mistry, Nilesh; Boer, Matthias; Schoendube, Harald; *Technical principles and phantom measurements evaluating HU accuracy and skin-line accuracy in the extended field of view (FOV) region in Computed Tomography (SW VB10 and VA20).* 2018 Siemens Healthineers White Paper

2. Cheung JP, Shugard E, Mistry N, Pouliot J, Chen J. Evaluating the impact of extended field-of-view CT reconstructions on CT values and dosimetric accuracy for radiation therapy. *Med Phys*. 2019;46(2):892-901. doi:10.1002/mp.13299

3. Ritter, Andre; Mistry, Nilesh; *Direct Density Technical Principles and implications for radiotherapy.* 2017Siemens Healthineers White Paper

CONTACT INFORMATION

For correspondence regarding this study, please contact Patricia Collins, PhD at PJG7C@hscmail.mcc.virginia.edu